RSC Advances

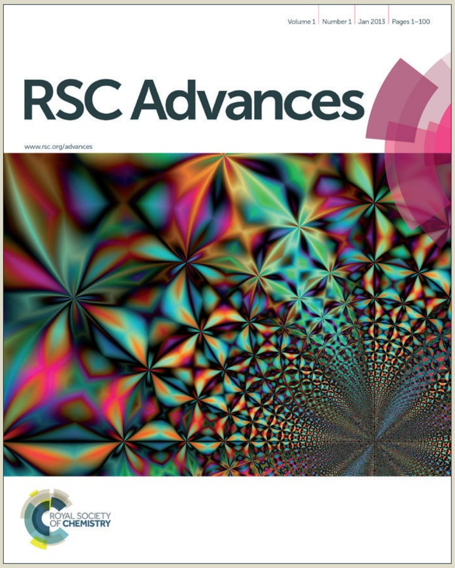

ROYAL SOCIETY OF CHEMISTRY

www.rsc.org/advances

Theoretical study on synergistic effects between anion–π and metal-Lp interactions

Meng Gao, Guanqing Gao, Qingzhong Li*, Xin Yang, Wenzuo Li, Jianbo Cheng

The Laboratory of Theoretical and Computational Chemistry, School of Chemistry and Chemical Engineering, Yantai University, Yantai 264005, People's Republic of China

Corresponding author:

Jianbo Cheng Dr

The Laboratory of Theoretical and Computational Chemistry

School of Chemistry and Chemical Engineering

Yantai University

Yantai 264005

People's Republic of China

Tel. (+086) 535 6902063

Fax. (+086) 535 6902063

E-mail: lqz@ytu.edu.cn

Abstract

This article investigated the interplay between the anion–π and coinage-metal–Lp interactions in the complexes involving three hetero-aromatic compounds of pyrazine, 1,4-dicyanobenzene and 1,4-benzoquinone. The physical nature of both interactions has been unveiled by means of molecular electrostatic potential and energy decomposition. Interesting cooperativity effects are observed when the anion–π and coinage-metal–Lp interactions coexist in the same multicomponent. These effects have been theoretically studied in terms of energetic and geometric features of the complexes as well as the charge transfer and orbital interactions. Weaker anion–π interaction shows a greater enhancement in the presence of stronger metal-Lp interaction. Additionally, experimental evidence for a combination of the two interactions was obtained from the Cambridge Structural Database.

Keywords: Anion–π interaction; Coinage-metal–Lp interaction; Cooperative effects

1. Introduction

Undoubtedly, non-covalent interactions are a key process in both chemistry and biochemistry. Among them, interactions including aromatic rings are of great importance in many areas including drug design,[1] crystal engineering and protein folding.[2] For example, π–π stacking,[3,4] cation–π,[5] anion–π,[6] CH–π,[7] and lone pair-π[8] interactions play a critical role in many important chemical and biological processes. Typically, anion–π interaction is a favorable noncovalent contact between an electron deficient (π–acidic) aromatic system and an anion. There were lots of experimental[9-13] and theoretical[14] researches for anion–π interactions, demonstrating that anion–π interaction plays a vital role in molecular recognition[15,16] and trans-membrane anion transport.[17] Abundant studies have revealed that anion–π interaction is generally dominated by electrostatic and anion-induced polarization contributions.[18-20]

It was known that the interactions including coinage metals play a key role in self-assembled monolayers[21,22] and organometallic complexes acting as efficient catalysts.[23,24] In 2003, Sadlej *et al.*[25] first proposed the concept of "X···Au-Y bridge". And then, abundant of studies occur for the complexes of coinage metals with lone-pair ligands.[26-28] In fact, the d^{10} coinage metal usually forms linear coordinate metal complexes with two ligands. Recently, the complexes formed by the coinage metal with lone-pair ligands including OX_2, NX_3, and PX_3 (X = H, F, and CH_3) have been analyzed and their stability is higher in order of Ag < Cu < Au.[28] Similarly, the metal-π interaction in complexes C_2H_4–MCN (M = Cu, Ag, and Au) also exhibits the same variation trend in stability.[29]

The importance of synergetic effect is based on the fact that the combination of weak intermolecular interactions of various sorts is helpful for accomplishing many chemical and biochemical processes including molecular recognition with high specificity and efficiency.[30-36] Interestingly, synergetic effect was found between anion-π and π-π interactions in complexes involving hexafluorobenzene where both interactions coexist, and the anion–π interaction imposes a strong influence on the π–π interaction.[32] Followed by this study, Deyà *et al.*[33] studied the interplay between anion–π and hydrogen bonding interactions in complexes involving aromatic rings. Very recently, Esrafile *et al.*[34] reported the mutual influence between anion-π and pnicogen bond interactions by *ab initio* calculations. Moreover, the weaker pnicogen bond has greater enhancement by the stronger anion–π interaction.[34] Similarly, interesting cooperative effects were found between anion–π and chalcogen bonding by this research group.[35] The presence of the anion–π interaction strengthens the chalcogen bond and the enhancement is related to the strength of chalcogen bond and the nature of anion.[35] More interestingly, we recently reported experimental and theoretical evidences for synergistic effects between cation-π and coinage-metal-oxygen interactions.[36] A synergetic effect was found with large cooperative energy, depending on the strengths of both interactions.[36] Given the above observation that the synergetic effect is present between different types of interactions, the question arises as to whether a cooperative effect can be found when anion-π and coinage metal-bonding interactions coexist in the same complex.

Hence, we selected three π–acidic hetero-aromatic compounds (**1**–**3**), shown in

Fig. 1, that contain substituent groups in the structures which can act as electron donors in coinage metal–Lp interactions. Fig. 2 indicates the schematic representation of isolated anion–π (**4-12**) and metal–Lp (**13-21**) as well as anion-π-metal–Lp bonded (**22-48**) complexes studied here. First, for the complexes **4-12** we study the nature of anion-π interaction and the influence of the anion on its strength. In the same way, we focus on the nature of coinage metal–Lp interaction and the dependence of its strength on the coinage metal and the lone-pair Lewis base in the complexes **13-21**. Finally, in the complexes **22-48** we pay our attention to the mutual influence between the two interactions as well as its relation with the nature of the anion, coinage metal and lone-pair Lewis base. To unveil the mechanism of synergistic effects, we perform an analysis of molecular electrostatic potentials and orbital interactions.

2. Computational details

All calculations were performed with the Gaussian 09 set of codes.[37] All complexes were optimized at the second-order Møller - Plesset perturbation theory (MP2) level with aug-cc-pVDZ basis set for all atoms except Cu, Ag and Au atoms. For the coinage metals, the aug-cc-pVDZ-PP basis set, which uses small-core relativistic pseudopotentials to describe the inner core orbitals, was adopted to account for relativistic effects. Optimization of complexes **4–48** was performed with imposition of C_{2v} symmetry to make them have similar structures, causing it possible to study the interplay between the two noncovalent interactions in the multicomponent systems. It has been demonstrated that such C_{2v} symmetry was often used when it is to study the interplay between anion-π and other type of interaction in the complexes involving **1-3** molecules.[33-35] It should be pointed out that most complexes with such C_{2v} symmetry except **13-18** are not minima.

Interaction energies were calculated using the supermolecular approach and corrected for the basis set superposition error (BSSE) using the counterpoise method proposed by Boys and Bernardi.[38] For the multicomponent systems, in which the anion-π interaction and the metal-bonding interactions coexist, the cooperative energy (E_{coop}) was evaluated with $E_{\mathrm{coop}} = \Delta E_{\mathrm{MULTI}} - \Delta E_{\text{anion-}\pi} - 2 \times \Delta E_{\text{M-Lp}} - \Delta E_{\text{anion-M}}$, where $\Delta E_{\mathrm{MULTI}}$, $\Delta E_{\text{anion-}\pi}$ and $\Delta E_{\text{M-Lp}}$ are the interaction energies of the corresponding optimized multi-component, anion–π, and metal-bonding, respectively. The last term ($\Delta E_{\text{anion-M}}$) is the interaction energy between the anion and MCN with the coordinates frozen in the geometries of the multi-components.

Charge transfer (CT) was calculated in terms of the natural population analysis (NPA) scheme via NBO 3.0 version[39] in the Gaussian 09 program. GAMESS program[40] was used to perform the energy decomposition analysis for the interaction energy with the LMOEDA method[41] at the MP2/aug-cc-pVDZ level. The topological analysis of the electron density for all complexes was performed by using Bader's theory of atoms in molecules (AIM) with the help of AIM2000 software[42] at the same level. Molecular electrostatic potentials (MEPs) on the 0.001 au contour of the electronic density were calculated by using the wavefunction analysis–surface analysis suite (WFA-SAS) program[43] at the MP2/aug-cc-pVDZ level.

3. Results and discussion

3.1 Energetic and geometric details of anion–π and metal–Lp complexes

Due to the electron-deficient nature of the three aromatic rings (**1-3**), they can form an anion-π interaction with anions. A symmetry of $C_{2,v}$ was exerted in the optimization of isolated anion–π (**4-12**) and metal–Lp (**13-21**) complexes. In Table 1 we listed the interaction energies and equilibrium distances of complexes **4-12** and **13-21**. The optimized equilibrium anion–π distances in the complexes **4–12** are in the range of 2.217–3.394 Å, which are comparable with the previous studies.[44] As expected, the equilibrium distances of anion–π interactions are longer with the increase of the anionic radius. For the given anion, a shorter distance is found for the anion–π interaction in the order of **1** > **2** > **3**. The interaction energy of anion–π interaction is related to the anion and hetero-aromatic ring. Specially, the interaction energy of anion–π interaction is more negative for the small anion. However, its dependence on the hetero-aromatic ring is complicated. For F^{-}, the anion–π interaction becomes stronger in the order of **1** < **2** < **3**, which is consistent with the most positive MEP on the ring central point in the π molecule (Table S1), while for Cl^{-} and Br^{-} the anion–π interaction is strengthened in the order of **1** < **3** < **2**, inconsistent with the change of binding distance. A reasonable explanation for this inconsistence will be given in the following energy decomposition.

To have a further insight into the nature of anion–π interaction, the interaction energy was decomposed into electrostatic energy (ES), exchange energy (EX), repulsion energy (REP), polarization energy (POL), and dispersion energy (DISP). The corresponding results are collected in Table 2. For the anion–π interaction in **4**, the value of POL is more than two times as much as that of both ES and DISP, whereas the three attractive terms (ES, POL, and DISP) have almost equivalent contributions to the anion–π interaction in **5** and **6** although the DISP term is a little greater. The small electrostatic energy in **4-6** is attributed to the fact that the pyrazine ring is not electron-deficient, confirmed by the small positive MEP on the ring central point in the π molecule (Table S1). However, the anion–π interaction involving pyrazine is compensated by the polarization term due to the small quadrupole moment of pyrazine (Q_{zz}=2.6 B).[45] Owing to the strong electron-withdrawing effect of CN and C=O groups, 1,4-dicyanobenzene and 1,4-benzoquinone become an electron-deficient ring, as shown in Fig. 1. Consequently, the electrostatic interaction is dominant in the anion–π interaction of complexes **7–12**. In addition, the π electron cloud of the aromatic ring has a bigger deformation due to the stronger polarizing power of F^{-}, thus the polarization energy is considerable in the complexes **7** and **10**. Also it is expected that the dispersion contribution grows up with the increase of the anionic radius. The shorter binding distance in the complexes **11** and **12** results in a bigger repulsion energy, which can be used to explain the contradiction that the complexes **11** and **12** exhibit a shorter binding distance but smaller interaction energy than **8** and **9**.

In Fig. 1, one can see a negative MEP on the nitrogen or oxygen atom in **1-3**, thus it is easy to understand the role of Lewis base for the oxygen or nitrogen in the O/N···MCN interaction (metal–Lp). Regarding metal–Lp complexes **13-21**, the interaction energies range from -17.99 to -46.77 kcal/mol, where some interesting results can be obtained. First, the compounds containing nitrogen atoms (**1** and **2**) form stronger metal-Lp complexes **13-18** than the oxygen-containing compound (**3**) in the complexes **19-21** because the nitrogen atom is a stronger Lewis base than the oxygen atom (Table S2). Second, pyrazine (**1**) forms a stronger metal-Lp interaction than 1,4-dicyanobenzene (**2**), although the negative MEP on the N atom in **1** is smaller than that in **2**. Clearly, this can be attributed to the higher electronegativity of the sp-hybridized nitrogen atom in **2**. Third, the dependence of metal-Lp interaction on the coinage metal is different for the different aromatic rings. For pyrazine, the metal-Lp interaction becomes stronger in the order of Ag < Cu < Au, in agreement with the previous study.[28] However, for 1,4-dicyanobenzene and 1,4-benzoquinone, the Cu complex is most stable, followed by the Au complex, and Ag forms the weakest complex. Antušek et al.[26] compared the influence of electron correlation effects and relativistic effects on the interaction energy of complexes between the coinage metal atoms (Cu, Ag, and Au) and lone-pair donating molecules (H_2O and NH_3). They pointed out that the interaction energy is mostly due to electron correlation effects, and the relativistic effects on the interaction energies are different for the ligand molecules.[26] Accordingly, the strength of coinage-metal-Lp interaction should be understood with a careful and comprehensive analysis of the role of the electron correlation and relativistic effects.

The energy decomposition analysis (EDA) shows that ES is more negative than IND and DISP in the coinage-metal–Lp bonded complexes (Table 2). This indicates that electrostatic interaction plays a dominant role in the formation of the coinage-metal-Lp interactions. Similarly, this conclusion was confirmed in the complexes of Y···AuCH$_3$ (Y = H_2O, CH_3OH, $(CH_3)_2O$).[46] ES is more negative in the coinage-metal–Lp interaction than that in the anion-π interaction, although the metal-Lp interaction has a covalent nature. For the coinage-metal–Lp interaction, the relatively large POL means that the molecular orbitals undergo significant changes in their shapes, which is typical in the formation of a covalent bond. The large EX indicates that there is a big overlap of orbitals between the two molecules in the coinage-metal-Lp bonded complexes, which is evidenced by the orbital interactions between the occupied orbitals in one molecule and the unoccupied ones in another molecule (Table S3). Simultaneously, the large EX results in a large REP in the coinage-metal–Lp bonded complexes due to the close contact.

The coinage-metal–Lp interaction is also analyzed with orbital interactions including $\mathrm{Lp}_{(N/O)}\rightarrow\mathrm{BD}^*_{(C\text{-}M)}$, $\mathrm{Lp}_{(N/O)}\rightarrow\mathrm{Lp}^*_{(M)}$, and $\mathrm{Lp}_{(M)}\rightarrow\mathrm{BD}^*_{(C\text{-}N/C\text{-}O)}$. Their magnitudes are estimated with the second-order perturbation energies (E^2) in Table S3. Although the charge back-donation interaction is also present in the coinage-metal-Lp interaction, characterized by the $\mathrm{Lp}_{(M)}\rightarrow\mathrm{BD}^*_{(C\text{-}N/C\text{-}O)}$ orbital interaction, it is much weaker than that in the coinage metal-π complex.[29] We think that the contribution of the charge back-donation interaction is marginal for the coinage-metal-Lp interaction. The relative magnitudes of both $\mathrm{Lp}_{(N/O)}\rightarrow\mathrm{BD}^*_{(C\text{-}M)}$ and $\mathrm{Lp}_{(N/O)}\rightarrow\mathrm{Lp}^*_{(M)}$ orbital interactions are pertinent to the coinage metal and the ligand molecules. For the Cu complexes, the $\mathrm{Lp}_{(N/O)}\rightarrow\mathrm{Lp}^*_{(M)}$ orbital interaction is much stronger than the $\mathrm{Lp}_{(N/O)}\rightarrow\mathrm{BD}^*_{(C\text{-}M)}$ one. However, a reverse result is found for the Au complexes. The $\mathrm{Lp}_{(N/O)}\rightarrow\mathrm{Lp}^*_{(M)}$ orbital interaction has comparable contribution to the Ag complexes

17 and **20** with the $\mathrm{Lp}_{(N/O)}\rightarrow\mathrm{BD}^*_{(C\text{-}M)}$ one, while the latter one is about two times as much as the former one in the Ag complex **14**.

Table 1 also lists the net charge transfer (CT) for the isolated anion-π and coinage-metal–Lp bonded complexes. Upon formation of **4-12** complexes, a net charge, in the range of 0.0044-0.0523e, transfers from the anion to the molecules **1-3**, which act as Lewis acids. In the complexes **12-21**, charge moves from the aromatic ring, being a Lewis base, to the MCN molecule. The largest CT occurs in the complex **15**, whereas the smallest CT is found in the complex **20**. A good linear relationship is found between the charge transfer and the interaction energy in the coinage-metal-Lp complexes (Fig. 3). This indicates that the charge transfer is important in the formation of coinage-metal–Lp complexes. In fact, the value of CT for the coinage-metal–Lp interaction is far larger than that in anion-π complexes, consistent with the nature of covalent interaction.

3.2. Cooperative effect between anion–π and coinage-metal–Lp interactions

The energetic results computed for the multicomponent complexes **22-48** (see Fig. 2) are summarized in Table 3. Clearly, both the anion-π and the coinage-metal-Lp interactions are strengthened each other in the complexes **22-48**, evidenced by the more negative interaction energies of both types of interactions. Moreover, the enhancement of the weak anion-π interaction is more prominent than that of the strong coinage-metal-Lp interaction. This conclusion is consistent with that found in other systems.[32-35] In addition, the enhancement of the anion-π interaction is dependent on the coinage-metal-Lp interaction and becomes larger in the order of

CuCN < AgCN < AuCN in most complexes except in **40-42**. These results show that there is positive cooperativity between the anion-π and the coinage-metal-Lp interactions, which is further evidenced by the negative cooperative energy (E_{coop}). This term provides an estimation of the "extra" energetic stabilization obtained in multicomponent complexes as a result of the coexistence of both interactions. For the Au complexes, E_{coop} is more negative than that in the other two coinage metal complexes. From Table 3, one can see that the E_{coop} value is smallest for the complex **28** because the increased percentage of the corresponding anion-π and metal-Lp interactions is smallest. Especially, the huge cooperative energy (-74.32 kcal/mol) is found in **42** since the monomer **3** has a great deformation in the complex.

Based on the important role of electrostatic interaction in the anion-π and metal-Lp interactions, we attempt to provide a rational explanation with molecular electrostatic potentials for the enhancement of both interactions in the multicomponent complexes **22-48**. One can see from Table S1 that the most positive MEP on the ring central point in the π molecule becomes larger in the complexes **13-21**. This means that the π molecule in **13-21** is a better electron acceptor in the anion-π interaction in comparison with that in the isolated molecules. Similarly, the presence of anion-π interaction enlarges the most negative MEP on the N/O atom in the anion-π complexes **4-12**. This indicates that the N/O atom in **4-12** becomes a better electron donor in the coinage-metal-Lp interaction than that of **1-3**. Moreover, the change of the negative MEP on the N/O atom is more prominent than that of the positive MEP on the ring central point.

The interplay between the anion-π and the coinage-metal-Lp interactions brings out a geometrical change in the complexes. One can see in Table S4 that the equilibrium distance of the anion-π interaction in **23-48** is much shorter than in the binary complexes **4-12**. That is, the presence of coinage-metal-Lp interaction greatly strengthens the anion-π interaction. However, the equilibrium distance of the coinage-metal-Lp interaction has slight change in the complexes **23-48** with respect to the complexes **13-21**. Namely, the presence of the anion-π interaction has a small effect on the strength of coinage-metal-Lp interaction.

Table S5 presents the charge transfer (CT) of anion-π and metal-Lp interactions in the multicomponent complexes **22-48** as well as its difference (ΔCT) with respect to the isolated anion-π and metal-Lp complexes. In **22-48**, the hetero-aromatic compounds act as both the Lewis acid (ring center) in the anion-π interaction and the Lewis base (N/O) in the metal-Lp interaction simultaneously. The direction of charge transfer is sequent in both types of interactions. So the value of ΔCT is positive in all complexes, indicating that the charge transfer is greater in **22-48** than that in **4-12** and **13-21**. Therefore, the positive ΔCT can be understood as an indication of reinforcement of the anion–π and metal-Lp interactions, in agreement with the negative cooperative energy. To study the relationship between charge transfer and cooperative effects, we plotted the map of the cooperative energy versus the change of charge transfer for the anion–π and metal-Lp interactions in Fig. S1. No good relation is found between the cooperative energy and the change of charge transfer for the anion–π interaction. This shows that the charge transfer in the anion–π interaction has a minor contribution to the cooperative energy. However, the charge transfer in the metal-Lp interaction has some responsibility for the cooperative energy since they have weak correlations.

To have a better understanding for the role of orbital interactions in enhancing the metal-Lp interaction, we analyzed the change of occupancy (Δn) on the selected orbitals in the complexes relative to the isolated molecules in Table S6. It is expected that the occupancy on the occupied orbitals is reduced and that on the vacant orbitals is increased. What is more, the change of occupancy becomes larger in order of Ag < Cu < Au, consistent with the strength of the metal-Lp interaction. The decrease of the occupancy on the N/O lone-pair orbital is more prominent than that on the metal lone-pair orbital. This confirms the secondary role of the charge back-donation interaction in the metal-Lp interaction. When the anion–π and metal-Lp interactions coexist in the same complex, the decrease of the occupancy on the N/O lone-pair orbital is larger, while that on the metal lone-pair orbital is smaller. In all, the orbital interactions in the metal-Lp interaction are stronger in **22-48**, resulting in a stronger metal-Lp interaction.

3.3. Experimental evidences

In order to obtain experimental evidences for the coexistence of the anion–π and coinage-metal-Lp interactions in crystal materials, searches in the Cambridge structural database (CSD)[47] were performed. Only crystal structures with no disorder and errors and R factors of less than 0.1 were considered. In exploring the CSD, we found some interesting structures. About 50 structures were found for pyrazine ring, while no related structures were found for **2** and **3** aromatic rings. Several selected crystal structures with the anion–π and coinage-metal-Lp interactions are shown in Fig. 4. The anions found in the crystal structures are often ClO_4^-, NO_3^-, BF_4^-, and PF_6^-. The coinage-metal atoms are directly adjoined with the N atoms of aromatic rings. In addition, the coinage-metal atoms are often silver and copper. Although these structures obtained by CSD research are not the same as those in our theoretical studies, they share some similarities in the coexistence of anion–π and M–Lp interactions. This provides a hint that the theoretical study for the interplay between anion–π and M–Lp interactions is helpful for constructing the corresponding crystal materials.

4. Conclusions

Ab initio calculations were performed to study the cooperative effects between the anion–π and coinage-metal–Lp interactions that coexist in the same complex. The equilibrium distances, interaction energies, charge transfer (CT) and the orbital occupancy were analyzed. It was found that both types of interactions are enhanced each other. Moreover, the weaker anion-π interaction shows a larger increased percentage of the interaction energy due to the presence of the stronger metal-Lp interaction. The calculated CT values of the anion-π and metal-Lp interactions in the multicomponent systems are greater than those in the isolated complexes, confirming the enhancement of both interactions. What is more, the crystal structures obtained by CSD survey indicate the coexistence of anion-π and metal-Lp interactions, and this demonstrates the potential applications with a combination of both interactions in crystal materials.

Acknowledgements

This work was supported by the Outstanding Youth Natural Science Foundation of Shandong Province (JQ201006), the Program for New Century Excellent Talents in University (NCET-2010-0923), and the Key Project of Natural Science Foundation of Shandong Province of China (ZR2013HZ004).

References

1 J. D. Hoheisel and D. Cahill, *Curr. Opin. Chem. Biol.*, 2002, **6**, 11–12.

2 E. A. Meyer, R. K. Castellano and F. Diederich, *Angew. Chem.*, 2003, **115**, 1244–1287.

3 C. Janiak, *J. Chem. Soc., Dalton Trans.*, 2000, **21**, 3885–3896.

4 J. T. Stivers and Y. L. Jiang, *Chem. Rev.*, 2003, **103**, 2729-2759.

5 J. C. Ma and D. A. Doufherty, *Chem. Rev.*, 1997, **97**, 1303–1324.

6 B. L. Schottel, H. T. Chifotides and K. R. Dunbar, *Chem. Soc. Rev.*, 2008, **37**, 68–83.

7 M. Nishio, Y. Umezawa, M. Hirota and Y. Takeuchi, *Tetrahedron*, 1995, **51**, 8665-8701.

8 M. Egli and S. Sarkhel, *Acc. Chem. Res.*, 2007, **40**, 197–205.

9 S. Demeshko, S. Dechert and F. Meyer, *J. Am. Chem. Soc.*, 2004, **126**, 4508–4509.

10 B. L. Schottel, J. Bacsa and K. R. Dunbar, *Chem. Commun.*, 2005, 46– 47.

11 I. A. Guralskiy, D. Escudero, A. Frontera, P. V. Solntsev, E. B. Rusanov, A. N. Chernega, H. Krautscheid and K. V. Domasevitch, *Dalton Trans.*, 2009, **15**, 2856–2864.

12 Y. J. Zhao, C. Beuchat, Y. Domoto, J. Gajewy, A. Wilson, J. Mareda, N. Sakai and S. Matile, *J. Am. Chem. Soc.*, 2014, **136**, 2101–2111.

13 M. V. Zlatović, S. Z. Borozan, M. R. Nikolić and S. D. Stojanović, *RSC Adv.*,

2015, **5**, 38361–38372.

14 D. Escudero, A. Frontera, D. Quiñonero, P. Ballester, A. Costa and P. M. Deyà, *J. Chem. Theory Comput.*, 2007, **3**, 2098–2107.

15 M. Mascal, *Angew. Chem. Int. Ed.*, 2006, **118**, 2956–2959.

16 M. Mascal, I. Yakovlev, E. B. Nikitin and J. C. Fettinger, *Angew. Chem. Int. Ed.*, 2007, **119**, 8938–8940.

17 V. Gorteau, G. Bollot, J. Mareda, A. Perez-Velasco and S. Matile, *J. Am. Chem. Soc.*, 2006, **128**, 14788–14789.

18 C. Garau, A. Frontera, D. Quioñero, P. Ballester, A. Costa and P. M. Deyà, *ChemPhysChem.*, 2003, **4**, 1344–1348.

19 D. Quioñero, C. Garau, C. Rotger, A. Frontera, P. Ballester, A. Costa and P. M. Deyà, *Angew. Chem., Int. Ed.*, 2002, **41**, 3389–3392.

20 D. Y. Kim, N .J. Singh and K. S. Kim, *J. Chem. Theory Comput.*, 2008, **4**, 1401–1407.

21 C. D. Bain, E. B. Troughton, Y. T. Tao, J. Evall, G. M. Whitesides and R. G. Nuzzo, *J. Am. Chem. Soc.* 1989, **111**, 321−335.

22 P. Maksymovych, O. Voznyy, D. B. Dougherty, D. C. Sorescu and J. T. Yates Jr., *Prog. Surf. Sci.*, 2010, **85**, 206−240.

23 N. Fey, A. G. Orpen and J. N. Harvey, *Bond. Coord. Chem. Rev.*, 2009, **253**, 704−722.

24 D. Manzoor, S. Krishnamurty and S. Pal, *J. Phys. Chem. C*, 2014, **118**, 7501−7507.

25 A. Avramopoulos, M. G. Papadopoulos and A. J. Sadlej, *Chem. Phys. Letts.*, 2003, **370**, 765−769.

26 A. Antušek, M. Urban and A. J. Sadlej, *J. Chem. Phys.*, 2003, **119**, 7247−7262.

27 J. Granatier, M. Urban and A. J. Sadlej, *J. Phys. Chem. A*, 2007, **111**, 13238−13244.

28 L. F. Pašteka, T. Rajský and M. Urban, *J. Phys. Chem. A*, 2013, **117**, 4472−4485.

29 M. Gao, X. Yang, J. B. Cheng, Q. Z. Li, W. Z. Li and R. E. Loffredo, *ChemPhysChem*, 2013, **14**, 3341–3347.

30 M. E. Alberto, G. Mazzone, N. Russo and E. Sicilia, *Chem. Commun.*, 2010, **46**, 5894–5896.

31 C. Garau, A. Frontera, D. Quiñonero, N. Russo and P. M. Deyà, *J. Chem. Theory Comput.*, 2011, **7**, 3012–3018.

32 A. Frontera, D. Quioñero, A. Costa, P. Ballester and P. M. Deyà, *New J. Chem.*, 2007, **31**, 556–560.

33 D. Escudero, A. Frontera, C. Estarellas, D. Quioñero and P. M. Deyà, *J. Comput. Chem.*, 2009, **30**, 75–82.

34 M. D. Esrafili, F. Mohammadian-Sabet and M. Solimannejad, *J. Mol. Graph. Model.*, 2015, **57**, 99–105.

35 H. A. Samimi, M. D. Esrafili, F. Mohammadian-Sabet and H. Haddadi, *Mol. Phys.*, 2015, **113**, 1442-1450.

36 M. Gao, Q. Z. Li, J. B. Cheng and W. Z. Li, *ChemPhysChem*, 2015, **16**, 1008–1016.

37 M. J. Frisch, G. W. Trucks, H. B. Schlegel, G. E. Scuseria, M. A. Robb, J. R. Cheeseman, G. Scalmani, V. Barone, B. Mennucci, G. A. Petersson, H. Nakatsuji, M. Caricato, X. Li, H. P. Hratchian, A. F. Izmaylov, J. Bloino, G. Zheng, J. L. Sonnenberg, M. Hada, M. Ehara, K. Toyota, R. Fukuda, J. Hasegawa, M. Ishida, T. Nakajima, Y. Honda, O. Kitao, H. Nakai, T. Vreven, J. A. Montgomery, Jr., J. E. Peralta, F. Ogliaro, M. Bearpark, J. J. Heyd, E. Brothers, K. N. Kudin, V. N. Staroverov, R. Kobayashi, J. Normand, K. Raghavachari, A. Rendell, J. C. Burant, S. S. Iyengar, J. Tomasi, M. Cossi, N. Rega, J. M. Millam, M. Klene, J. E. Knox, J. B. Cross, V. Bakken, C. Adamo, J. Jaramillo, R. Gomperts, R. E. Stratmann, O. Yazyev, A. J. Austin, R. Cammi, C. Pomelli, J. W. Ochterski, R. L. Martin, K. Morokuma, V. G. Zakrzewski, G. A. Voth, P. Salvador, J. J. Dannenberg, S. Dapprich, A. D. Daniels,. Farkas, J. B. Foresman, J. V. Ortiz, J. Cioslowski and D. J. Fox, *Gaussian 09, Revision A.02*, Gaussian, Inc., Wallingford CT, 2009.

38 S.F. Boys and F. Bernardi, *Mol. Phys.*, 1970, **19**, 553–566.

39 A. E. Reed, L. A. Curtiss and F. Weinhold, *Chem. Rev.*, 1988, **88**, 899–926.

40 M. W. Schmidt, K. K. Baldridge, J. A. Boatz, S. T. Elbert, M. S. Gordon, J. H.

Jensen, S. Koseki, N. Matsunaga, K. A. Nguyen, S. J. Su, T. L. Windus, M. Dupuis and J. A. Montgomery, *J. Comput. Chem.*, 1993, **14**, 1347–1363.

41 P. F. Su and H. Li, *J. Chem. Phys.*, 2009, **13**, 014102.

42 R. F. W. Bader, AIM2000 Program, v 2.0, McMaster University, Hamilton, Canada, 2000.

43 F. A. Bulat, A. Toro-Labbé, T. Brinck, J. S. Murray and P. Politzer, *J. Mol. Model.*, 2010, **16**, 1679–1691.

44 C. Estarellas, A. Frontera, C. Estarellas, D. Quioñero and P. M. Deyà, *ChemPhysChem*, 2011, **12**, 2742–2750.

45 C. Garau, A. Frontera, D. Quinonero, P. Ballester, A. Costa and P. M. Deya, *J. Phys. Chem. A*, 2004, **108**, 9423–9427

46 Q. Z. Li, H. Li, B. Jing, R. Li, Z. B. Liu, W. Z. Li, F. Luan, J. B. Cheng, B. A. Gong and J. Z. Sun, *Chem. Phys. Lett.*, 2010, **498**, 259–262.

47 F. H. Allen, *Acta. Crystallogr. B*, 2002, **58**, 380–388.

Table 1 Interaction energy corrected for BSSE (Δ*E*, kcal/mol), equilibrium distance (*R*, Å), electron density (ρ, au), Laplacian ($\nabla^2\rho$, au), energy density (*H*, au), and charge transfer (CT, e) in the complexes

Complexes	Δ*E*	*R*	ρ	$\nabla^2\rho$	*H*	CT
4(**1**+F$^-$)	-5.11	2.663	0.0086	0.0435	0.0018	0.0095
5(**1**+Cl$^-$)	-4.49	3.240	0.0063	0.0237	0.0007	0.0074
6(**1**+Br$^-$)	-3.94	3.394	0.0060	0.0215	0.0006	0.0075
7(**2**+F$^-$)	-16.26	2.572	0.0090	0.0428	0.0018	0.0044
8(**2**+Cl$^-$)	-12.88	3.147	0.0069	0.0240	0.0006	0.0047
9(**2**+Br$^-$)	-11.90	3.300	0.0066	0.0219	0.0005	0.0048
10(**3**+F$^-$)	-17.74	2.217	0.0121	0.0629	0.0029	0.0523
11(**3**+Cl$^-$)	-11.35	3.011	0.0081	0.0269	0.0008	0.0291
12(**3**+Br$^-$)	-10.01	3.196	0.0076	0.0234	0.0006	0.0283
13(**1**+2CuCN)	-43.63	1.843	0.1265	0.6074	-0.0534	0.2258
14(**1**+2AgCN)	-31.02	2.090	0.0947	0.4320	-0.0219	0.1854
15(**1**+2AuCN)	-46.77	2.032	0.1228	0.4799	-0.0471	0.2744
16(**2**+2CuCN)	-42.45	1.777	0.1395	0.7183	-0.0634	0.2252
17(**2**+2AgCN)	-28.58	2.038	0.0993	0.4909	-0.0239	0.1642
18(**2**+2AuCN)	-41.71	1.974	0.1315	0.5602	-0.0542	0.2322
19(**3**+2CuCN)	-28.47	1.807	0.1086	0.7709	-0.0260	0.1742
20(**3**+2AgCN)	-17.99	2.119	0.0677	0.4241	-0.0026	0.1004
21(**3**+2AuCN)	-25.24	2.064	0.0869	0.5340	-0.0119	0.1478

Note: *R* is the distance between the central point of the ring and the anion in the anion-π interaction and the distance between the metal atom and the lone-pair atom in the metal-Lp interaction. Topological parameters correspond to the cage critical point (CCP) in the anion-π interaction and the bond critical point (BCP) in the metal-Lp interaction. CT is the absolute value of the sum of charge on all atoms of the heteroaromatic ring in the anion-π interaction and the sum of charge on all atoms of the heteroaromatic ring in the metal-Lp interaction.

Table 2 Electrostatic energy (ES), exchange energy (EX), repulsion energy (REP), polarization energy (POL), dispersion energy (DISP), and interaction energy (Δ*E*) in the complexes at the MP2/aug-cc-pVDZ level. All are in kcal/mol.

Complexes	ES	EX	REP	POL	DISP	Δ*E*
4	-5.19	-22.58	36.50	-11.06	-4.93	-7.26
5	-4.43	-20.12	31.84	-5.62	-6.63	-4.96
6	-4.98	-20.93	33.19	-4.76	-6.88	-4.36
7	-16.67	-27.82	45.28	-14.63	-2.62	-16.47
8	-14.78	-25.57	40.83	-7.78	-5.81	-13.11
9	-15.11	-26.67	42.70	-6.61	-6.40	-12.09
10	-31.25	-52.53	89.78	-21.69	-2.73	-18.43
11	-18.82	-34.53	56.74	-9.37	-5.78	-11.76
12	-18.19	-33.99	55.90	-7.87	-6.27	-10.42
13	-65.14	-72.75	146.13	-27.04	-23.30	-42.09
14	-51.09	-66.76	129.02	-23.91	-16.56	-29.30
15	-65.21	-91.27	178.38	-47.62	-19.13	-44.85
16	-60.55	-73.26	147.70	-31.20	-23.27	-40.57
17	-47.22	-64.01	123.77	-25.20	-14.16	-26.81
18	-58.69	-89.08	173.76	-49.29	-16.40	-39.69
19	-41.77	-49.70	99.87	-21.93	-13.66	-27.18
20	-29.00	-36.22	69.26	-14.00	-7.17	-17.12
21	-35.49	-49.24	94.24	-25.05	-8.38	-23.91

Table 3 Total interaction energy ($\Delta E_{\mathrm{total}}$, kcal/mol), interaction energies of anion-π ($\Delta E_{\mathrm{anion\text{-}\pi}}$), metal-Lp interaction ($\Delta E_{\mathrm{M\text{-}Lp}}$), and cooperative energy (E_{coop}, kcal/mol) in the complexes **22-46** as well as their increased percentage (%) relative to the complexes **4-21**.

Complexes	$\Delta E_{\mathrm{total}}$	$\Delta E_{\mathrm{anion\text{-}\pi}}$	%	$\Delta E_{\mathrm{M\text{-}Lp}}$	%	E_{coop}
22(**1**+2CuCN+F^-)	-136.89	-12.83	151	-46.36	6	-6.27
23(**1**+2AgCN+F^-)	-111.97	-14.92	192	-34.74	12	-8.19
24(**1**+2AuCN+F^-)	-143.23	-18.26	257	-52.18	12	-11.54
25(**1**+2CuCN+Cl^-)	-127.51	-9.26	106	-45.66	5	-3.25
26(**1**+2AgCN+Cl^-)	-102.91	-10.66	137	-33.78	9	-4.65
27(**1**+2AuCN+Cl^-)	-133.84	-13.73	205	-51.01	9	-7.55
28(**1**+2CuCN+Br^-)	-125.08	-8.43	114	-45.54	4	-2.71
29(**1**+2AgCN+Br^-)	-100.50	-9.51	141	-33.54	8	-3.88
30(**1**+2AuCN+Br^-)	-131.43	-12.50	218	-50.71	8	-6.61
31(**2**+2CuCN+F^-)	-129.11	-25.77	59	-47.27	11	-9.29
32(**2**+2AgCN+F^-)	-101.92	-27.05	66	-33.96	19	-10.41
33(**2**+2AuCN+F^-)	-127.56	-29.21	80	-48.26	16	-12.72
34(**2**+2CuCN+Cl^-)	-122.23	-20.49	59	-46.30	9	-7.34
35(**2**+2AgCN+Cl^-)	-95.15	-21.71	69	-32.99	15	-8.44
36(**2**+2AuCN+Cl^-)	-120.65	-23.67	84	-47.18	13	-10.54
37(**2**+2CuCN+Br^-)	-120.28	-19.03	60	-46.10	9	-6.85
38(**2**+2AgCN+Br^-)	-93.24	-20.22	70	-32.77	15	-7.93
39(**2**+2AuCN+Br^-)	-118.70	-22.13	86	-46.93	13	-9.97
40(**3**+2CuCN+F^-)	-129.53	-37.02	109	-33.80	19	-19.43
41(**3**+2AgCN+F^-)	-107.27	-29.93	69	-18.41	2	-11.18
42(**3**+2AuCN+F^-)	-174.92	-96.03	441	-52.63	109	-74.32
43(**3**+2CuCN+Cl^-)	-103.37	-21.63	91	-33.68	18	-9.17
44(**3**+2AgCN+Cl^-)	-80.27	-21.92	93	-23.07	28	-9.04
45(**3**+2AuCN+Cl^-)	-95.00	-24.81	119	-31.75	26	-11.82
46(**3**+2CuCN+Br^-)	-100.56	-20.03	100	-33.76	19	-8.96
47(**3**+2AgCN+Br^-)	-77.50	-20.43	104	-23.16	29	-8.89
48(**3**+2AuCN+Br^-)	-91.84	-26.07	160	-31.71	26	-11.17

Figure captions

Fig. 1 Schematic representation and molecular electrostatic potentials of three heteroaromatic rings

Fig. 2 Anion-π complexes, metal-Lp complexes, and anion-π-metal-Lp complexes

Fig. 3 Relationship between the charge transfer (CT) and the interaction energy of metal-Lp interaction ($\Delta E_{\text{metal-Lp}}$)

Fig. 4 Partial views of the crystal structures corresponding to XAYNIU, FUCTAY, JECDUQ, and OHEQIC

Figure 1

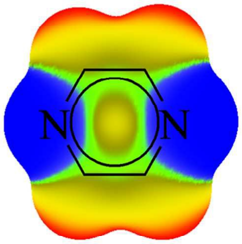

1

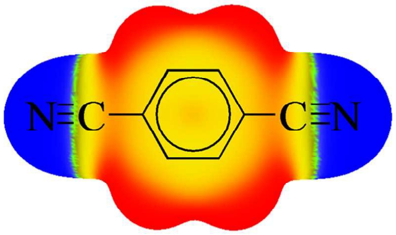

2

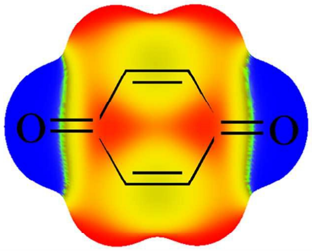

3

Figure 2

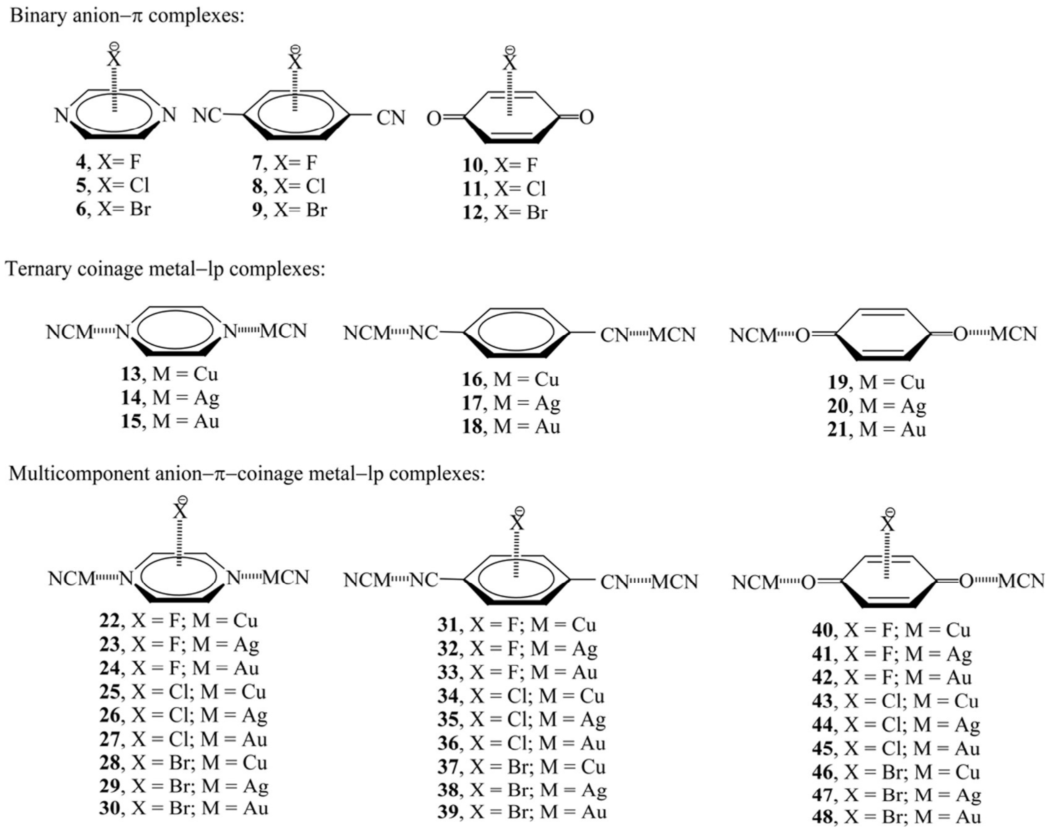
Binary anion−π complexes:
X
N
N
NC
CN
O
O
4, X= F
5, X= Cl
6, X= Br
7, X= F
8, X= Cl
9, X= Br
10, X= F
11, X= Cl
12, X= Br
Ternary coinage metal−lp complexes:
NCM N N MCN
NCM NC CN MCN
NCM O O MCN
13, M = Cu
14, M = Ag
15, M = Au
16, M = Cu
17, M = Ag
18, M = Au
19, M = Cu
20, M = Ag
21, M = Au
Multicomponent anion−π−coinage metal−lp complexes:
X
NCM N N MCN
NCM NC CN MCN
NCM O O MCN
22, X = F; M = Cu
23, X = F; M = Ag
24, X = F; M = Au
25, X = Cl; M = Cu
26, X = Cl; M = Ag
27, X = Cl; M = Au
28, X = Br; M = Cu
29, X = Br; M = Ag
30, X = Br; M = Au
31, X = F; M = Cu
32, X = F; M = Ag
33, X = F; M = Au
34, X = Cl; M = Cu
35, X = Cl; M = Ag
36, X = Cl; M = Au
37, X = Br; M = Cu
38, X = Br; M = Ag
39, X = Br; M = Au
40, X = F; M = Cu
41, X = F; M = Ag
42, X = F; M = Au
43, X = Cl; M = Cu
44, X = Cl; M = Ag
45, X = Cl; M = Au
46, X = Br; M = Cu
47, X = Br; M = Ag
48, X = Br; M = Au

Figure 3

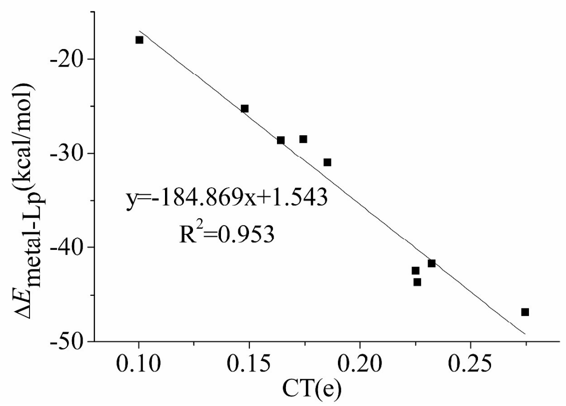
$\Delta E_{\text{metal-Lp}}$(kcal/mol)
-20
-30
-40
-50
0.10
0.15
0.20
0.25
CT(e)
y=-184.869x+1.543
R^2=0.953

Figure 4

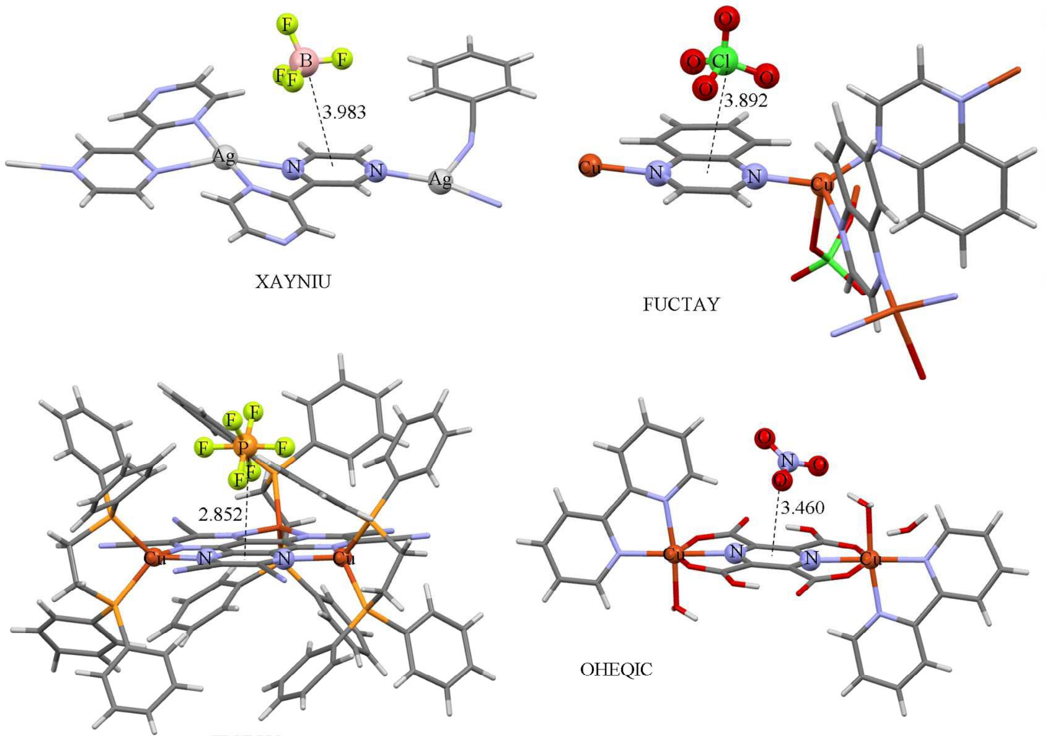

XAYNIU

FUCTAY

JECDUQ

OHEQIC

TOC

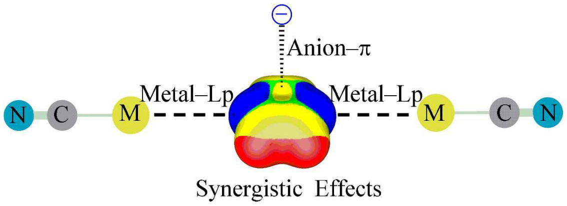

Interesting cooperativity effects are observed when the anion–π and coinage-metal–Lp interactions coexist in the same multicomponent.